LiHoF$_4$: Cuboidal demagnetizing factor in an Ising ferromagnet

M. Twengström [1], L. Bovo [2,3] O. A. Petrenko,[4] S. T. Bramwell,[2] and P. Henelius[1,5]

[1]*Department of Physics, Royal Institute of Technology, SE-106 91 Stockholm, Sweden*

[2]*London Centre for Nanotechnology and Department of Physics and Astronomy, University College London,*
17-19 Gordon Street, London WC1H OAH, United Kingdom

[3]*Department of Innovation and Enterprise, University College London, 90 Tottenham Court Road, Fitzrovia,*
London W1T 4TJ, United Kingdom

[4]*Department of Physics, University of Warwick, Coventry CV4 7AL, United Kingdom*

[5]*Faculty of Science and Engineering, Åbo Akademi University, 20500 Turku, Finland*

The demagnetizing factor can have an important effect on physical properties, yet its role in determining the behavior of nonellipsoidal samples remains to be fully explored. We present a detailed study of the role of spin symmetry in determining the demagnetizing factor of cuboids, focusing, as a model example, on the Ising dipolar ferromagnet LiHoF$_4$. We distinguish two different functions: the demagnetizing factor as a function of intrinsic susceptibility $N(\chi)$ and the demagnetizing factor as a function of temperature $N(T)$. For a given nonellipsoidal sample, the function $N(\chi)$ depends only on dipolar terms in the spin Hamiltonian, but apart from in the limits $\chi \to 0$ and $\chi \to \infty$, it is a different function for different spin symmetries. The function $N(T)$ is less universal, depending on exchange terms and other details of the spin Hamiltonian. We apply a recent theory to calculate these functions for spherical and cuboidal samples of LiHoF$_4$. The theoretical results are compared with $N(\chi)$ and $N(T)$ derived from experimental measurements of the magnetic susceptibility of corresponding samples of LiHoF$_4$, both above and below its ferromagnetic transition at $T_c = 1.53$ K. Close agreement between theory and experiment is demonstrated, showing that the intrinsic susceptibility of LiHoF$_4$ and other strongly magnetic systems can be accurately estimated from measurements on cuboidal samples. Our results further show that for cuboids, and implicitly for any sample shape, $N(\chi)$ below the ordering transition takes the value $N(\infty)$. This confirms and extends the scope of earlier observations that the intrinsic susceptibility of ferromagnets remains divergent below the transition, in contradiction to the implications of broken symmetry. We discuss the topological and microscopic origins of this result.

I. INTRODUCTION

The demagnetizing energy of a magnetized sample presents several intriguing aspects. It plays a crucial role in the analysis of magnetic susceptibility [1,2], realizes a laboratory example of long-range interactions [3], and even mediates some exotic physics, for example, the complex nonlinear response and pattern formation in the intermediate state of type-I superconductors [4]. In view of the pioneering work of Poisson, Maxwell, and others, the "demagnetizing effect" may at first sight appear to be a solved problem that belongs to the textbooks, but a closer appraisal of the literature reveals that it remains, to this day, a rather rich source of mathematical and practical challenges [5–8]. As far as magnetic materials are concerned, demagnetizing effects and corrections are

particularly important in the discussion of several phenomena that are dominated by long-range interactions, including, for example, magnetic monopole excitations in the spin ices [9], topological skyrmionic spin textures [10], and spintronic applications of antiferromagnets [11]. Even the problem of how to calculate the demagnetizing factor for shapes beyond ellipsoids is far from being solved in any general sense: many years of investigation have yielded some particularly elegant results [12,13], and ongoing work has revealed new surprises. In a recent study [3] we noted an unexpected dependence of the demagnetizing factor on the microscopic aspects of the material for rectangular prismatic samples, in contrast to the long-held expectation that only shape and macroscopic susceptibility should be relevant [5]. In this paper we elucidate this effect in detail with respect to a real model system: the Ising-like dipolar ferromagnet LiHoF$_4$.

We therefore focus on a fundamental property of magnetism, namely, the response to a small applied magnetic field: the intrinsic isothermal magnetic susceptibility, $\chi = \lim_{H \to 0} \partial M / \partial H$, where M is the magnetization and H is the internal magnetic field. The susceptibility is a fundamental thermodynamic characteristic of a magnetic system, reflecting its microscopic nature and magnetic state. With very careful

measurement, it can reveal surprising properties, as exemplified in our recent detection of "special temperatures" in frustrated magnets [14]. Compared to more local probes of spin correlations such as neutron scattering or muon relaxation, bulk susceptibility measurements offer the advantage of relative experimental simplicity and precise control of the experimental environment. However, there are still important aspects that one must consider in order to obtain a truly accurate measurement of the intrinsic material susceptibility. Many materials of recent interest contain high-moment rare-earth ions leading to a high susceptibility ($\chi \geqslant 1$) and consequent strong demagnetizing effects. The state of the system can then be defined and determined only after particularly careful corrections for such effects.

In detail, it is well known that the internal magnetization and magnetic field of a paramagnetic ellipsoid exposed to an external magnetic field are uniform within the sample. The demagnetizing field H_d is given by $H_d = -NM$, where M is the magnetization and N is the demagnetizing factor (more generally, this is a tensor relationship $H_d^\alpha = -N^{\alpha\beta}M_\beta$). Remarkably, N, as defined in one direction, depends solely on the geometry of the sample and is independent of any underlying material properties. Due to the nature of the long-range dipolar interaction, the internal fields become nonuniform for nonellipsoids, and the calculation of the demagnetizing factors becomes a much more complex task. However, at an early point it was realized that it is possible to define a demagnetizing factor for cuboids that depends not only on the sample geometry but also on the intrinsic susceptibility $\chi(T)$, which leads to the temperature dependence of N [15,16]. Another avenue of research focused on the approximation of uniform magnetization, from which useful results were derived [13,17]. Interestingly, the temperature-dependent N for cuboids has not been applied much in practice, although many experiments are performed on cuboids. This is despite the fact that the χ dependence of N was calculated [5,6] nearly 20 years ago using a finite-element method to solve the field equations. We and coworkers more recently introduced an alternative, iterative microscopic method, along with a brute-force Monte Carlo calculation [3], and the predicted χ dependence of N was also supported by direct measurements on cuboids of the spin ice compound $Dy_2Ti_2O_7$. However, as already mentioned, in addition to the χ dependence of N, Ref. [3] further discovered a dependence on the microscopic symmetry of the spin. For example, an isotropic Heisenberg spin system or isotropic multiaxial Ising systems such as $Dy_2Ti_2O_7$ feature a different N from a uniaxial Ising system. In this study we test this theory using cuboids of the uniaxial Ising compound $LiHoF_4$ and find that the theory accounts for the experimentally determined N very well.

II. EXPERIMENTAL METHOD

$LiHoF_4$ (see Fig. 1) is an insulating rare-earth dipolar ferromagnet [18]. Due to the low-lying orbitals of the magnetic Ho^{3+} ions, the dipolar interaction is stronger than the exchange interaction, and the material orders magnetically at a relatively low critical temperature of $T_c \approx 1.53$ K [19]. Significant crystal fields lead to a strong uniaxial Ising anisotropy
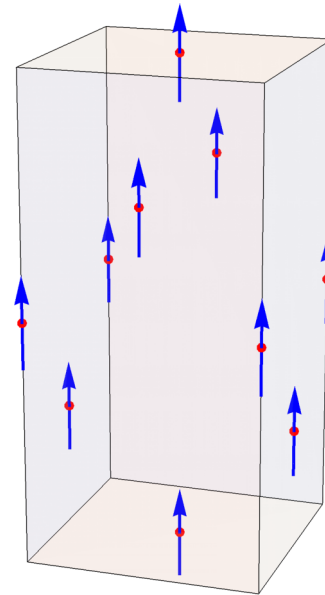

FIG. 1. The conventional unit cell of lithium holmium tetrafluoride ($LiHoF_4$). The red dots represent the holmium ion positions, and the blue arrows indicate the Ising-like spins of $LiHoF_4$ when fully magnetized along its principal (*c*) axis.

with the Ising direction aligned with the principal axis of the tetragonal unit cell containing four Ho^{3+} ions, with a magnetic moment of about $7\mu_B$ per ion. Due to the relative simplicity of the effective model [20], the possibility to dilute the material with nonmagnetic Y^{3+} ions [21], and its sensitivity to applied transverse magnetic fields, $LiHoF_4$ has been used in numerous studies on classical and quantum phase transitions [22,23] and slow magnetic dynamics [24].

The crucial aspect of $LiHoF_4$ for this study is its uniaxial Ising symmetry, which distinguishes it from the isotropic, multiaxial Ising spin ice compound $Dy_2Ti_2O_7$ used in our previous study [3]. In addition, we benefited from the commercial availability of $LiHoF_4$ aligned single-crystal samples cut to a range of shapes and aspect ratios that would have been challenging to realize in a laboratory (or in house) given the brittle nature of this material. In this investigation we consider spherical, cubic, long, and needle-shaped samples of $LiHoF_4$, with dimensions given in Table I. The cuboidal samples were grown, cut, aligned, and polished by Altechna, and we checked their alignment and crystal quality by x-ray

TABLE I. Physical dimensions of samples used. Error bars are ∼0.03 mm on dimensions and 1 in the last stated digit on weights. The last two columns contain the calculated demagnetizing factors in the limit of zero and infinite susceptibility for each sample.

Shape	Dimensions (mm)	Weight (g)	$N(\chi = 0)$	$N(\chi = \infty)$
Sphere	$\varnothing = 3.8$	0.16415	1/3	1/3
Cube	$4.08 \times 3.87 \times 4.09$	0.36505	0.327	0.274
Long	$1.95 \times 2.17 \times 8.10$	0.19235	0.110	0.0751
Needle	$0.60 \times 0.67 \times 8.05$	0.01773	0.0363	0.0197

Laue diffraction. Note that that the "cube" was not perfectly cubic, a difference that was accounted for in the analysis. The spherical sample was derived from a sample supplied by Altechna that was further hand cut as in Ref. [14]. It was accurately aligned along the crystalline c axis (the easy axis of magnetization) by applying a 7 T magnetic field in a viscous liquid grease at room temperature and then cooling to solidify the grease. In general, the best estimate for the volume (used to determine the susceptibility) was calculated through the weight and the density, $\rho = 5.72$ g/cm^3.

The magnetic susceptibility was studied on different instruments in two temperature regimes, $T \geqslant 1.8$ K and $T \leqslant 2$ K.

At $T \gtrsim 1.8$ K, the magnetic moment for each sample was measured as a function of temperature using a Quantum Design superconducting quantum interference device (SQUID) magnetometer, where the samples were positioned in a cylindrical plastic tube to ensure a uniform magnetic environment. Fields of 15 and 25 Oe were applied, and there was no detectable nonlinearity of the susceptibility in this range. Measurements were performed in the reciprocating sample option operating mode to achieve improved sensitivity by eliminating low-frequency noise. For the cuboids we initially trusted the design specifications and used the cuboid edges as reference for alignment in the magnetometer (our x-ray study later showed one sample to have edges that were slightly misaligned with its crystal axes, as discussed subsequently). By analogy with Ref. [25], different measurements were made: low-field susceptibility and field-cooled versus zero-field-cooled susceptibility, with no significant differences observed. Also, magnetic field sweeps up to several hundred oersteds at fixed temperature were performed in order to evaluate the susceptibility accurately, to confirm the linear approximation, and to estimate the absolute susceptibilities, following the method described in our previous work [25].

The magnetic moment at lower temperatures was measured using a different Quantum Design magnetic property measurement system SQUID magnetometer equipped with an *i*Quantum ^{3}He insert [26]. The applied fields were 50 and 100 Oe.

Data between the high- and low-temperature regimes have been compared, in particular in the overlapping region $1.8 \leqslant T \leqslant 2$ K. Without further manipulation, the two sets of data are in very good agreement with variations of the order of 1%. This variation can be attributed to several factors, including the uncertainty in the actual field value in each of the two instruments (due in part to the presence of small frozen fields in the superconducting coils) and variations in precise sample positioning within the pickup coils. Here we show only data below 5 K.

The field, measured in oersteds, and the magnetic moment m, measured in emu, were converted into SI units using

$$\chi_{\text{SI}} = \frac{4\pi m[\text{emu}]}{H[\text{Oe}]V[\text{cm}^3]}. \tag{1}$$

III. THEORY OF THE DEMAGNETIZING FACTOR

The theory that we apply is given in detail in Ref. [3], but it is useful to summarize some of its key aspects here.

Textbook presentations of the demagnetizing factor emphasize how the homogeneity of the internal field and local magnetization for ellipsoids allows one to define a demagnetizing factor N for a specified crystal axis. This is a fixed number for any given ellipsoid: for example, the exact demagnetizing transformation for a sphere ($N = 1/3$) is

$$\frac{1}{\chi} = \frac{1}{\chi_{\text{exp, sphere}}} - \frac{1}{3}, \tag{2}$$

where $\chi_{\text{exp, sphere}} = \partial M/\partial H_0$ is the experimentally determined susceptibility and H_0 is the uniform applied magnetic field.

This is typically contrasted with the case of nonellipsoids, where neither internal field nor magnetization are uniform, with the consequence that a demagnetizing factor N can no longer be defined as a unique, fixed number in the way it can for ellipsoids. Nevertheless, for our purposes, it is most important to stress the fact that a temperature-dependent demagnetizing factor $N(T)$ can still be precisely defined for any sample shape.

To see this, consider an arbitrarily shaped sample, subject to the field H_0. The incremental magnetic work is $\mu_0 H_0 \mathrm{d}m$, where $m = MV$ is the magnetic moment of the sample of volume V, which uniquely defines the magnetization M. We can then write

$$\frac{1}{\chi} = \frac{1}{\chi_{\text{exp, ne}}} - N, \tag{3}$$

where $N(T)$ is the demagnetizing factor of the nonellipsoidal (ne) sample, which corresponds to the standard "magnetometric" demagnetizing factor for simple shapes like cylinders or rectangular prisms.

It can then be seen by eliminating χ from Eqs. (2) and (3) that $N(T)$ is the quantity that precisely maps the temperature dependence of the magnetic moment of the nonellipsoid onto that of the sphere or any arbitrary ellipsoid. Hence, a knowledge of $N(T)$ allows the measurement of χ for any sample shape. In the fundamental investigation of magnetic materials, χ is the quantity of interest as it can be calculated, in principle, from a knowledge of the spin Hamiltonian or simulated numerically using periodic boundaries and Ewald methods. Here, the thermodynamic limit is taken in regards to the change in the surface term stemming from the fluctuations of the magnetic moments which produce a surface charge. The full derivation was made by de Leeuw *et al.* [27] using a semiclassical approach, and a thorough microscopic derivation can be found in Ref. [28].

For a system with inhomogeneous fields, it is therefore still possible to precisely define $N(T)$ without making explicit reference to the inhomogeneities. They do, however, continue to play a crucial role in determining the numerical value $N(T)$ at each temperature. For a given χ, our iterative method accounts for the inhomogeneity spin by spin and can be implemented on any given spin structure or local spin symmetry (Ising, XY, Heisenberg) for system sizes up to about $\mathcal{N} = 10^6$ spins. We supplement it by direct, brute-force,

Monte Carlo simulations of the spin Hamiltonian, and in both cases extrapolate to the thermodynamic limit, $\mathcal{N} \to \infty$. In Ref. [3] we and colleagues showed that the thermodynamic limit values of $N(T)$ are in excellent agreement for the two methods, even though the finite-size corrections are rather different.

We believe that these methods go beyond previous approaches in that the viewpoint is no longer mesoscopic (i.e. "micro"magnetic in the common notation) but, rather, is truly microscopic and spin Hamiltonian based. Hence, it is more appropriate for certain fundamental studies, such as that of spin ice [3] and LiHoF$_4$, studied here. This conclusion does not detract from the value of the micromagnetic approaches for many magnetic problems, and we have demonstrated complete agreement between our approach and that of Chen *et al.* [5,6] in the case of cubic spin ice.

Indeed, the works of Chen *et al.* have revealed many important features of the problem: notably, for cylinders (and we can expect the same for cuboids), as $\chi \to 0$, the demagnetizing field is nonuniform, but the magnetization is uniform [29]. Hence, in that limit, using the results of Ref. [13], the cube has the same demagnetizing factor as a sphere, $N = 1/3$. In the opposite limit, $\chi \to \infty$, the roles are reversed, and the demagnetizing field is uniform (on some mesoscopic scale), but the magnetization is nonuniform [29]. So for a cube, N takes a different limiting value, $N \approx 0.27$. Our work identifies aspects of the behavior of the function $N(\chi)$ between these two limits.

In our method, we first determine the function $N(\chi)$, which depends only on the definition of the spin degrees of freedom and their dipole-dipole interactions and, importantly, is independent of exchange terms in the spin Hamiltonian. Then, by substituting $\chi(T)$ into $N(\chi)$, the new function $N(T)$ is determined, and it is at this point that the full details of the spin Hamiltonian enter into the problem. Hence, all relevant terms in the spin Hamiltonian affect $N(T)$, but only dipolar terms affect $N(\chi)$.

The effect of anisotropy terms in the spin Hamiltonian is rather subtle. They will, in general, affect the bulk susceptibility tensor and, through that, the demagnetizing tensor and demagnetizing factor $N(\chi)$ in a way that is compatible with the crystal symmetry. For example, spin ice has local Ising spins, but its space symmetry is cubic. Hence, the local Ising terms are not manifest in the function $N(\chi)$, which is the same as that of other isotropic systems. However, they do strongly affect the temperature dependence of $\chi(T)$ and, through that, the function $N(T)$.

For the uniaxial spin system studied in this paper and for a given sample shape, $N(\chi)$ will be a different function than that of cubic spin ice because the susceptibility tensor has different symmetry, although it will coincide in the limit $\chi \to 0$, where the magnetization becomes homogeneous, and also, it seems [3], in the limit $\chi \to \infty$, where the demagnetizing field becomes homogeneous (see above). It is in this rather subtle way, where $N(\chi)$ and $N(T)$ are both affected, but to different degrees, that microscopic effects—in particular the effects of local spin symmetry—may be revealed in the behavior of the demagnetizing factor for nonellipsoidal samples, such as the cuboids studied here.
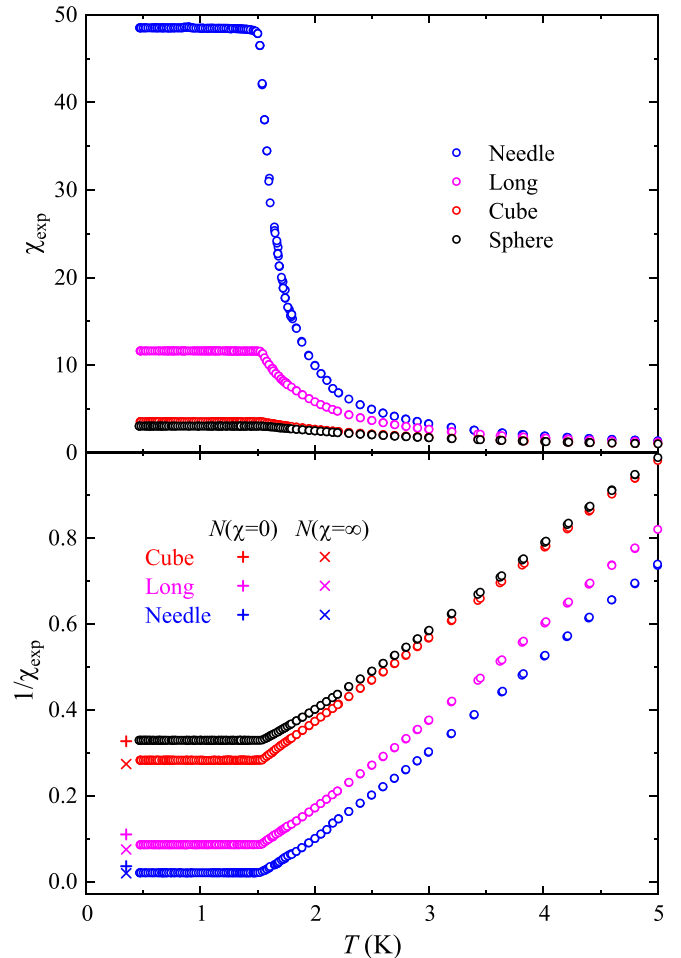

FIG. 2. The experimentally measured susceptibility (top panel) and inverse susceptibility (bottom panel) as a function of temperature T for the differently shaped samples of LiHoF$_4$ listed in Table I. The lower plot also shows $\chi \to 0$ and $\chi \to \infty$ values of $N(\chi)$ from the tables of Ref. [6].

IV. RESULTS

In Fig. 2 (top panel) we show the measured low-temperature susceptibility of the different samples and note that the shape dependence dominates the susceptibility.

The inverse susceptibility, shown in Fig. 2 (bottom panel), is very reminiscent of Fig. 2 in the detailed early study of Cooke *et al.* [30]. The low-T plateau in the inverse susceptibility below the critical temperature of the material is expected to occur at the value of the demagnetizing factor N for the sample (see Sec. V). The low-T susceptibility thus provides direct experimental access to the demagnetizing factor for ferromagnets. The estimated $\chi \to 0$ and $\chi \to \infty$ values of N [5,6], indicated respectively by color-coded pluses and crosses on the graph, are compared to the low-temperature plateau of the susceptibility for each sample. The $\chi \to \infty$ values are significantly closer to experiment, a first significant result that we return to below in Sec. V.

For the spherical sample we would expect the plateau exactly at $\chi = 1/N = 3$, while it is a bit higher, $\chi = 3.037$, possibly due to a deviation from a perfectly spherical shape. The slope in the limit of high temperature should be identical

for all samples since it is related to the Curie constant of the material. The gradients of the inverse susceptibility in the 4–4.5 K interval are similar for the sphere and cube (0.211 and 0.215, respectively) but higher for the long sample and needle (0.233 and 0.228, respectively). This discrepancy is larger than what our theory can account for. We considered two possible origins of the discrepancy. First, we investigated a possible misalignment between the local Ising axis and the long side of the cuboids. A Laue camera measurement showed the misalignment to be 5° and 6° for the long and needle samples, respectively. However, this degree of misalignment cannot easily explain a 7%–9% error in the susceptibility. Second, we considered the effect of finite sample dimensions leading to a systematic error in the assumed point dipole approximation, as discussed by Stamenov and Coey [31]. Room temperature measurement of palladium foil samples, shaped to match our LiHoF4 sample dimensions (Table I), revealed a ∼7% error (on the low side) in the measured susceptibility of only the long and needle samples. It seems safe to conclude that the observed discrepancies of 7% and 9% largely have this origin, with a small contribution from misalignment. While it would have been ideal to use much shorter samples, such samples would have also had to be very thin to preserve their aspect ratios, and this would have made them very fragile. Hence, rather than use shorter samples, we make a correction to the susceptibilities, as described below.

If the demagnetizing factor happened to be independent of temperature, as many studies assume, all the curves in Fig. 2 (bottom) should simply be vertically shifted images of each other, as can be deduced from the classical demagnetizing transformation

$$\frac{1}{\chi} = \frac{1}{\chi_{\mathrm{exp}}} - N. \tag{4}$$

However, in Fig. 2, we clearly see that this is not valid for the spherical and cuboidal samples since the curves start to diverge at low temperature. These temperature-dependent deviations from the usual demagnetizing transformation are the main subject of this study.

Since the demagnetizing factor for the sphere is independent of the temperature, we can find the intrinsic susceptibility of the material using Eq. (4) with $N = 1/3.037 = 0.3293$ in the present case. Using the intrinsic susceptibility, we then obtain the temperature-dependent demagnetizing factor N for the other samples using Eq. (4).

The main result of this study is shown in Fig. 3, where we see the experimentally determined N as a function of T for the samples of Table I compared to several theoretical predictions. The upper red circles denote the experimentally derived $N(T)$ for the cubic sample, compared to our calculation for an Ising system (solid line, calculation given in Ref. [3]), the commonly assumed T-independent value of 1/3 (dashed line, equal to $N(\chi \to 0)$), and the theoretical prediction for an isotropic Heisenberg system [3,5,6] (dotted line). It is confirmed that the calculation of Ref. [3] is fully consistent with the experimental result, while the T-independent value and Heisenberg result both differ significantly from it. In Fig. 3 further results are displayed for the long and needle samples. For the long sample, the agreement between experiment and our theory is very satisfactory, while the T-independent
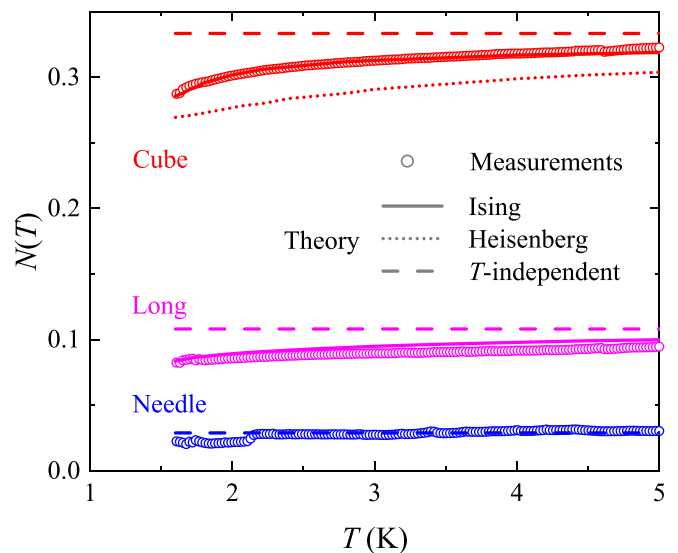

FIG. 3. Temperature dependence of the experimentally derived demagnetizing factor $N(T)$ for the approximate cube of LiHoF4 (red circles) as well as for the long sample (magenta circles) and the needle sample (blue circles). These are compared to theoretical predictions (lines with the same color code) specified in the legend. Our prediction for Ising spins accounts for the experimental data very accurately, while other predictions fail, except for the needle sample.

($\chi \to 0$) theory fails to describe experiment. For the needle sample, the difference between theories is small, and the data confirm that the T-independent theory works reasonably well, while the sample geometry in this case precluded a reliable calculation by our method.

In order to determine $N(T)$ for the long sample and needle, we multiplied the susceptibilities by factors 1.09 and 1.07, respectively, to ensure that the slope of $\chi(T)$ approaches the same high-T limit, which is a physical requirement. As noted above, we believe that the main source of this deviation is a correction to the point dipole approximation in the magnetization measurement [31].

To emphasize the importance of accurate demagnetizing transformations when the susceptibility is large, like it is for many rare-earth-based magnets at low temperature, we show in Fig. 4 the result of determining the intrinsic material susceptibility from the measurement on the cube. In black, we show the reference intrinsic susceptibility determined from the sphere, using $N = 0.3293$. For comparison, we have transformed the measurement on the cube in three different ways: using the theory for uniaxial Ising spins (red solid line), the theory for Heisenberg spins (red dotted line), and the frequently used approach of assuming the high-susceptibility value of $N = 1/3$ (red dashed line). As Fig. 4 illustrates, the theory for uniaxial Ising spins reproduces the reference susceptibility very well, while the theory for Heisenberg spins underestimates the susceptibility considerably—by more than 50% at the lowest temperature. This would cause unacceptable errors in, say, the determination of a critical exponent for the transition. Similarly, the T-independent transformation diverges at $\chi_{\mathrm{exp}} = 3$, which would falsely indicate a critical temperature of $T_c = 1.8$ K, well above the actual $T_c = 1.53$ K.
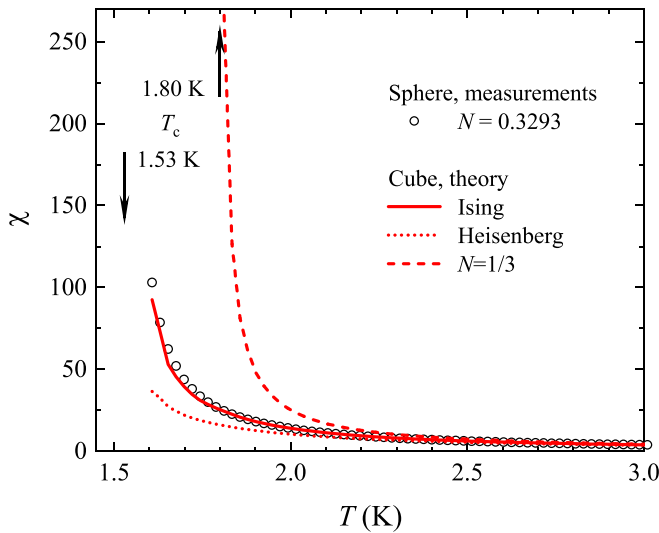
FIG. 4. Experimental intrinsic susceptibility of LiHoF$_4$ derived under different assumptions about the behavior of the demagnetizing factor for the cubic sample. The true value is determined from the susceptibility of the sphere using $N = 0.3293$ (black circles), and this is compared with that derived from the cube using several theories: our theory for uniaxial Ising spins (red solid line), the theory for Heisenberg spins (red dotted line), and the commonly used, T-independent value of $N = 1/3$ (red dashed line). It can be seen that the use of an incorrect demagnetizing factor leads to unacceptable errors in the derived intrinsic susceptibility. The plot also contrasts the apparent $T_c = 1.80$ K implied by the T-independent curve with the correct $T_c = 1.53$ K, corresponding to the divergence of the Ising curve.

V. DISCUSSION AND CONCLUSION

In summary, the demagnetizing transformation for an ellipsoid involves a single number that depends only on sample shape. For a nonellipsoidal sample the transformation is still well defined but becomes much more subtle. Taking a cubic sample as an example, in the small-χ limit, the transformation is (surprisingly) the same as that of a sphere, $N = 1/3$, and in the large-χ limit, it reaches a number that does not depend on any microscopic details of the spin Hamiltonian. Between these limits, as we have demonstrated by comparing experiment to microscopic theory, $N(\chi)$ depends on the underlying microscopic symmetry of the magnetic moment of the material. In Fig. 3, it is confirmed that the measured demagnetizing factor N for the nearly cubic sample of LiHoF$_4$ is accurately accounted for by our theory, which takes the symmetry of the spin and the T-dependence into account, while the measurement differs from both the T-dependent result for an isotropic material [3,5,6] and the T-independent, small-χ value. In Fig. 4, we see that this seemingly small difference in N has a very significant effect on the final transformed intrinsic susceptibility of the material, the aim of most susceptibility measurements.

It is clear that use of an ellipsoidal sample, where the temperature-independent demagnetizing factor is known, is a robust way to accurately determine the intrinsic susceptibility of a material. We note that early measurements of critical exponents on LiHoF$_4$ [32] and, for example, the rare-earth

dipolar magnets RCl$_3$ · 6H$_2$O (R = Dy, Er) [33] and dysprosium ethyl sulfate [34] did, indeed, employ ellipsoidal samples, so there is no reason to doubt their conclusions. Earlier studies on nonellipsoidal samples may contain systematic errors, but the results presented here show how accurate intrinsic susceptibilities can be estimated from magnetization data on cuboidal samples. These results therefore have practical relevance to any experimental technique where the demagnetizing factor needs to be considered: for example, neutron diffraction, nuclear magnetic resonance (NMR), muon spin rotation (μSR), x-ray magnetic circular dichroism (XMCD), and magneto-optical Kerr effect (MOKE), to list a few. However, it should also be noted that such results for single crystals do not easily translate through to powder samples: in a compacted pellet, for example, the demagnetizing field will depend on both the overall shape and any internal grain boundaries or voids. Estimating it accurately would be a difficult, though interesting, challenge. Hence, measurements on single-crystal samples, if available, are always preferable when demagnetizing effects are large.

Our measurements at temperatures below T_c confirm that the magnetic moment of the cuboidal samples remains remarkably constant, at the value $m = H_0 V / N(\chi = \infty)$. This may be simply derived by setting the internal field to zero in the equation

$$H_{\text{int}} = H_0 - NM. \tag{5}$$

Indeed, it is a well-known property of many (typically "soft") ferromagnets that was discussed theoretically many years ago [35–37]. It appears that the closest to an explanation of this experimental fact was that found by Wojtowicz and Rayl [36], who considered a highly idealized model of a toroidal sample, where a perpendicular ordering field competes with a curling mode within the plane of the toroid: in that case, a mean-field treatment yielded the observed behavior. This is an interesting result as it suggests a topological origin to the experimental observation of constant moment. However, in the present case of a uniaxial magnet it is difficult to make the same argument as the low-temperature state is not a curling mode but, rather, a complex domain state. In early studies of several uniaxial systems including LiHoF$_4$ (see Ref. [30] and references therein), it was proposed that domain wall movement is sufficiently free that domains move so that the average demagnetizing field exactly cancels the applied field. Certainly, if the response is confined to the movement of purely macroscopic objects (the domain walls), this would be associated with effectively zero entropy change per spin and hence athermal behavior. If the free energy is equated to the demagnetizing energy $E = (\mu_0 V / 2) N M^2$, then $\chi_{\text{exp}} = 1/N$, as observed.

However, for nonellipsoidal samples, this raises the question as to which demagnetizing factor to use in the calculation of the moment. Our results (Fig. 2, bottom panel) show conclusively that it is, indeed, the $\chi = \infty$ value of $N(\chi)$, as calculated here and in Refs. [5,6], rather than the usual $\chi = 0$ value. As predicted in Ref. [38], the paramagnetic fluctuations seem to anticipate the low-temperature domain structure.

This result strongly indicates that $\chi = \infty$ for all $T \leqslant T_c$, regardless of sample shape. In turn, it raises a certain ambiguity as to what χ represents in the ordered phase. If χ is interpreted as the susceptibility for $N = 0$, then one has to

admit that it should be finite below T_c because of the broken symmetry of the ferromagnetic state. On the other hand, if it is defined as in Fig. 3 to be a property of a sphere (say), then it can be infinite as a property of the spherical domain state. As the temperature is lowered below T_c, the domain magnetization will increase, and the domain susceptibility will decrease, consistent with a dipolar ordering transition [22,32], but the bulk intrinsic susceptibility will remain infinite. The infinite susceptibility, or "critical line," at all temperatures below T_c is reminiscent of a topologically ordered Kosterlitz-Thouless phase [39] or of a soft mode (infinite transverse susceptibility) in an ordered, continuously degenerate system. In view of the Wojtowicz-Rayl argument [36], where the ferromagnetic transition is accompanied by the appearance of a global topological defect (the winding mode of a torus), and the infinite susceptibility as $N \to 0$ does arise from a soft mode, such analogies are worth considering. A detailed numerical study of domain patterns in LiHoF$_4$ revealed a preference for a structure of parallel (to c) sheets of alternately spin "up" and spin "down" [40]. The infinite susceptibility could then reflect the free motion of smooth or rough domain walls that restore symmetry (at least locally) between spin-up and spin-down ordered states. There is, indeed, a certain topological character to the phenomenon as domain walls can be classified as topological defects, and rough ones can even map microscopically to the Kosterlitz-Thouless phase (although the evidence is that the long-range interaction suppresses roughness in LiHoF$_4$ [41]). Further investigation of the topological origins of the flat susceptibility of ferromagnets would certainly be worthwhile.

The insights of Ref. [36] further defined the "kink point" method of measuring the spontaneous magnetization as a function of temperature. At the "kink" temperature T_k where the magnetic moment becomes "flat," the vanishing of the internal field, coupled with the continuity of the magnetic moment versus temperature curve, suggests that the spontaneous magnetization $M_s(T_k)$ is given by $M_s(T_k) = H_0/N$. By varying H_0, one can determine the function $M_s(T)$ and hence

the critical exponent β (see, for example, Ref. [34]). It is not clear whether this property will precisely survive in the case of a nonellipsoidal sample because even though the internal field is zero and the magnetic moment is continuous with temperature, the magnetization itself is nonuniform even in the high-temperature phase (see Sec. III). Hence, although corrections to the kink point method may not be very large, it should be applied with caution when nonellipsoidal samples are used.

It is indeed worth emphasizing that the corrections to the demagnetizing transformation that we have identified are, of course, indicative of inhomogeneous fields within the sample. Such inhomogeneities are likely to be macroscopic, with details on length scales that are not much shorter than the sample dimensions [40]. Thus, diffuse magnetic neutron scattering, which measures generalized susceptibilities on rather smaller scales, is not likely to be strongly affected by these corrections, but magnetic Bragg scattering will be strongly affected—a fact that will need to be accounted for in neutron scattering studies of ordered states. In general, from the perspective of magnetic moment measurement, field inhomogeneities represent a correction to be transformed away, but from a more general perspective, they are an interesting phenomenon in their own right and can be precisely analyzed, as we have illustrated in this paper.

[1] E. C. Stoner, Philos. Mag. **36**, 803 (1945).

[2] J. A. Osborn, Phys. Rev. **67**, 351 (1945).

[3] M. Twengström, L. Bovo, M. J. P. Gingras, S. T. Bramwell, and P. Henelius, Phys. Rev. Mater. **1**, 044406 (2017).

[4] R. Prozorov, R. W. Giannetta, A. A. Polyanskii, and G. K. Perkins, Phys. Rev. B **72**, 212508 (2005).

[5] D.-X. Chen, E. Pardo, and A. Sanchez, IEEE Trans. Magn. **38**, 1742 (2002).

[6] D.-X. Chen, E. Pardo, and A. Sanchez, IEEE Trans. Magn. **41**, 2077 (2005).

[7] M. Beleggia, M. De Graef, and Y. T. Millev, Philos. Mag. **86**, 2451 (2006).

[8] G. Di Fratta, Proc. R. Soc. A **472**, 20160197 (2016).

[9] C. Castelnovo, R. Moessner, and S. L. Sondhi, Nature **451**, 42 (2008).

[10] N. Nagaosa and Y. Tokura, Nat. Nanotechnol. **8**, 899 (2013).

[11] T. Jungwirth, J. Sinova, A. Manchon, X. Marti, J. Wunderlich, and C. Felser, Nat. Phys. **14**, 200 (2018).

[12] G. Rowlands, J. Magn. Magn. Mater. **118**, 307 (1993).

[13] P. Rhodes and G. Rowlands, Proc. Leeds Philos. Lit. Soc., Sci. Sec. **6**, 191 (1954).

[14] L. Bovo, M. Twengström, O. A. Petrenko, T. Fennell, M. J. P. Gingras, S. T. Bramwell, and P. Henelius, Nat. Commun. **9**, 1999 (2018).

[15] J. Würschmidt, Z. Phys. **12**, 128 (1923).

[16] F. von Stäblein and H. Schlechtweg, Z. Phys. **95**, 630 (1935).

[17] R. I. Joseph and E. Schlömann, J. Appl. Phys. **36**, 1579 (1965).

[18] M. J. P. Gingras and P. Henelius, J. Phys.: Conf. Ser. **320**, 012001 (2011).

[19] G. Mennenga, L. J. deJongh, and W. J. Huiskamp, J. Magn. Mater **44**, 59 (1984).

[20] P. B. Chakraborty, P. Henelius, H. Kjønsberg, A. W. Sandvik, and S. M. Girvin, Phys. Rev. B **70**, 144411 (2004).

[21] D. H. Reich, T. F. Rosenbaum, and G. Aeppli, Phys. Rev. Lett. **59**, 1969 (1987).

[22] J. A. Griffin, M. Huster, and R. J. Folweiler, Phys. Rev. B **22**, 4370 (1980).

[23] D. Bitko, T. F. Rosenbaum, and G. Aeppli, Phys. Rev. Lett. **77**, 940 (1996).

[24] A. Biltmo and P. Henelius, Nat. Commun. **3**, 857 (2012).

[25] L. Bovo, L. D. C. Jaubert, P. C. W. Holdsworth, and S. T. Bramwell, J. Phys.: Condens. Matter **25**, 386002 (2013).

[26] N. Shirakawa, H. Horinouchi, and Y. Yoshida, J. Magn. Magn. Mater. **272–276**, e149 (2004).

[27] S. W. de Leeuw, J. W. Perram, and E. R. Smith, Proc. R. Soc. London, Ser. A **373**, 27 (1980).

[28] J. W. Perram and E. R. Smith, J. Stat. Phys. **46**, 179 (1987).

[29] D.-X. Chen, J. A. Brug, and R. B. Goldfarb, IEEE Trans. Magn. **27**, 3601 (1991).

[30] A. H. Cooke, D. A. Jones, J. F. A. Silva, and M. R. Wells, J. Phys. C **8**, 4083 (1975).

[31] P. Stamenov and J. M. D. Coey, Rev. Sci. Instrum. **77**, 015106 (2006).

[32] P. Beauvillain, J. P. Renard, I. Laursen, and P. J. Walker, Phys. Rev. B **18**, 3360 (1978).

[33] E. Lagendijk and W. J. Huiskamp, Physica (Amsterdam) **65**, 118 (1973).

[34] R. Frowein and J. Kotzler, Z. Phys. B **25**, 279 (1976).

[35] A. Arrott, Phys. Rev. Lett. **20**, 1029 (1968).

[36] P. J. Wojtowicz and M. Rayl, Phys. Rev. Lett. **20**, 1489 (1968).

[37] R. B. Griffiths, Phys. Rev. **188**, 942 (1969).

[38] W. Wasilewski, Phys. Lett. A **84**, 80 (1981).

[39] J. M. Kosterlitz and D. J. Thouless, J. Phys. C: Solid State Phys. **6**, 1181 (1973).

[40] A. Biltmo and P. Henelius, Europhys. Lett. **87**, 27007 (2009).

[41] G. I. Mias and S. M. Girvin, Phys. Rev. B **72**, 064411 (2005).